POLITECNICO DI TORINO
Repository ISTITUZIONALE

A temperature-aware battery cycle life model for different battery chemistries

Original
A temperature-aware battery cycle life model for different battery chemistries / Bocca, Alberto; Sassone, Alessandro; Shin, Donghwa; Macii, Alberto; Macii, Enrico; Poncino, Massimo (IFIP ADVANCES IN INFORMATION AND COMMUNICATION TECHNOLOGY). - In: VLSI-SoC: Design for Reliability, Security, and Low Power / Shin Y., Tsui C.Y., Kim J.J., Choi K., Reis R.. - STAMPA. - [s.l] : Springer International Publishing, 2016. - ISBN 978-3-319-46096-3. - pp. 109-130 [10.1007/978-3-319-46097-0_6]

Availability:
This version is available at: 11583/2650390 since: 2020-02-25T11:07:13Z

Publisher:
Springer International Publishing

Published
DOI:10.1007/978-3-319-46097-0_6

Terms of use:

This article is made available under terms and conditions as specified in the corresponding bibliographic description in the repository

Publisher copyright
Springer postprint/Author's Accepted Manuscript

This version of the article has been accepted for publication, after peer review (when applicable) and is subject to Springer Nature's AM terms of use, but is not the Version of Record and does not reflect post-acceptance improvements, or any corrections. The Version of Record is available online at: http://dx.doi.org/10.1007/978-3-319-46097-0_6

(Article begins on next page)

12 October 2024

A Temperature-Aware Battery Cycle Life Model for Different Battery Chemistries

Alberto Bocca[1], Alessandro Sassone[1], Donghwa Shin[2], Alberto Macii[1], Enrico Macii[1], and Massimo Poncino[1]

[1] Politecnico di Torino, Corso Duca degli Abruzzi 24, 10129 Italy
{alberto.bocca,alessandro.sassone,alberto.macii enrico.macii,massimo.poncino}@polito.it
[2] Yeungnam University, 280 Daehak-Ro, Gyeongsan, Gyeongbuk 712-749, Republic of Korea
donghwashin@yu.ac.kr

Abstract. With the remarkable recent rise in the production of battery-powered devices, their reliability analysis cannot disregard the assessment of battery life. In the literature, there are several battery cycle life models that exhibit a generic trade-off between generality and accuracy.
In this work we propose a compact cycle life model for batteries of different chemistries. Model parameters are obtained by fitting the curve based on information reported in datasheets, and can be adapted to the quantity and type of available data. Furthermore, we extend the basic model by including some derating factors when considering temperature and current rate as stress factors in cycle life.
Applying the model to various commercial batteries yields an average estimation error, in terms of the number of cycles, generally smaller than 10%. This is consistent with the typical tolerance provided in the datasheets.

Keywords: Battery modeling, cycle life, battery chemistry, capacity fading.

1 Introduction

Rechargeable batteries are an essential component in many application domains, such as electric vehicles, mobile systems, renewable energy, and telecommunication systems. In order to carry out an early verification of these systems, including the exchange of energy between the energy storage devices and other components, it becomes essential to have accurate and efficient battery models, especially models that evaluate the lifetime of the battery in terms of useful charge-discharge cycles.
In the literature various models for different functional aspects of batteries have been proposed, with differing tradeoffs between accuracy and generality. In the field of electronic design, the most commonly used ones are those in which the battery is described by a generic standard model expressed in terms of an *equivalent electrical circuit*. (e.g., [1, 2]). This is then populated either using data obtained from direct measurements on actual devices or by extrapolation of battery characteristics available from datasheets (e.g., [3]). These kinds of models are typically generated for a specific battery chemistry and show a high degree of accuracy. This accuracy may significantly degrade if

these models are applied to different battery chemistries. Furthermore, they are specific to a given battery chemistry and thus show a very high degree of accuracy. Obviously, this degree of accuracy can vary (decrease) significantly if the model, generated for a particular battery chemistry, is applied to batteries with different chemical characteristics.

On the other hand, in certain contexts (e.g., automotive, aerospace, smart grids), designers often rely on simpler compact analytical macromodels, such as Peukert's law [4], as a quick estimator for the sizing of the battery sub-system or for preliminary what-if analysis. These macromodels are aimed at the generation of a general relationship between the battery *intra-cycle* runtime and the most relevant parameters, like the Depth of Discharge (DOD) or State of Charge (SOC) of a battery.

While these models have reasonable generality (e.g., they can be applied to various batteries with different chemical characteristics, once characterized), they are focused on a single charge/discharge cycle of a battery. They do not provide information about the "lifetime" of a battery, i.e, decrease in performance due to long-term *inter-cycle* effects, such as the fading of the total capacity (ampere-hour) caused by repeated cycling. It is possible to incorporate such aging effects into these circuit-level or analytical models, for instance by replacing the use of a fixed battery capacity value with a generic function of some parameters. However, this operation requires (i) an understanding of the various phenomena that affect battery aging, and (ii) the construction of a compact model that can be used either as a standalone model or incorporated in traditional functional battery models.

The literature provides several studies on these effects, proposing mathematical models that are based on the electrochemical properties or the physics of the batteries and are therefore strongly bound to specific battery materials and chemistry (e.g., [5–9]). Although some other aging models, such as those proposed in [10–15], are empirically characterized onto a pre-defined equation template, they are still derived by measurements and, therefore, are not general enough to support different battery chemistries.

The objective of this work is the generation of an aging model with similar characteristics to a Peukert-like equation. This should be (i) analytical, but able to be empirically populated, and (ii) general enough to support different battery chemistries. Specifically, we propose a mathematical model for estimating the number of cycles with respect to the related capacity fade of batteries.

The accuracy of the approach proposed is demonstrated by applying this model to various commercial batteries of different chemistries, for which the manufacturers provide information on the long-term effects in their datasheets. The results show an average estimation error, referring to the number of cycles, generally within 10%, which is consistent with the typical tolerance provided in various datasheets (e.g., [16]).

The paper is organized as follows. Section 2 reports related works on battery modeling, while Section 3 describes the proposed mathematical model for estimating the number of cycles of batteries, and Section 4 reports the experimental results. In addition, Section 5 reports the proposed model extended to the temperature and current effects on battery aging, with the related results, while Section 6 draws some conclusions.

2 Background and motivations

2.1 Battery Aging Issues

The life degradation of a rechargeable battery depends on some irreversible changes of physical, mechanical, and chemical nature (e.g., [17],[18] for lithium-ion batteries) in its basic components, such as (i) corrosion, cracking, plating, or exfoliation of the electrodes, (ii) decomposition of the electrolyte and/or of the binder, and (iii) corrosion of the separator, just to list the most evident ones.
The most tangible effect of such deterioration is the irreversible reduction of the total battery capacity, which is named *capacity fade*. This fading in capacity is often measured by the so-called state-of-health (SOH), calculated as the ratio between the actual total capacity C_{aged} and the rated capacity C_R (i.e., the total capacity of one fresh battery), as reported in (1), while the difference C_R - C_{aged} defines the capacity loss (i.e., C_{fade}). In this case, most manufacturers provide information on fading as a percentage (i.e., in a normalized form).

$$SOH = \frac{C_{aged}}{C_R} \tag{1}$$

Battery aging is largely determined by:

- **Temperature (T)**. As with other typical reliability mechanisms, aging usually increases with increasing temperatures; as energy generation process in the battery involves a chemical reaction, the relation with temperature follows an Arrenhius-type of equation. Section 5.1 describes the main temperature effects on cycle life, from a battery perfomance point of view.
- **Depth-of-Discharge (DOD)**. The DOD is the percentage of battery capacity that has been discharged before starting a new charge phase. A DOD of 100% implies that a battery has been fully discharged before starting a new charge phase. Aging increases with deeper discharge cycles (i.e., higher DOD values).
- **Charge/discharge current**. Both currents affect battery degradation, but generally with a different impact on aging (e.g., [19]). Aging worsens with larger charge or discharge currents. Impact of a certain current on aging strictly depends on the battery chemistry and temperature. Section 5.2 faces this issue considering an analysis for various batteries.
- **Number of cycles (N)**. In a given cycle, deterioration mainly depends on the working and operating conditions. In addition, it may also depend on the number of charge/discharge cycles previously encountered or, in other terms, on the battery SOH at which a certain cycle is performed.

2.2 Battery Aging Models

Although various models have been proposed in literature, they usually have many parameters whose values have to be empirically extracted from direct analysis. For instance, [5] proposes an aging model for a certain lithium-ion (Li-ion) battery that relies on crack propagation theory, with some battery specific constants also related to mechanical strain. It further includes the average state-of-charge (SOC) in the model, since

battery aging generally increases for high average SOC values. However, although that mathematical comprehensive model is well-known in the literature, there are practical difficulties to adapt it to different Li-ion batteries.
Concerning cycle life estimation, numerous researchers have proposed analytical models capturing the main aging mechanisms and capacity fading based on the electrochemical properties of the batteries and even including full-physics based models (e.g., [8] for Li-ion batteries). In fact, the causes for degradation in batteries generally differs when considering the various cell components (e.g., electrolyte chemical composition, electrodes design, and active material) [17]. However, from the perspective of an electronic designer this modeling approach is unfeasible and, therefore, more simple and generic aging models are searched. In this work, we focus on compact mathematical battery cycle life models with only a couple of parameters in their formulas, other than the aforementioned aging factors (e.g., DOD and N).
In [9] the authors proposed a model to calculate the usable number of cycles N of a battery based on the following equation:

$$N = N_1 \cdot e^{\alpha \cdot (1 - DOD')} \tag{2}$$

where DOD' is the normalized depth of discharge ($0 \leq DOD' \leq 1$), α is a characteristic constant of the battery and N_1 is the number of cycles at $DOD' = 1$. This model is empirically characterized for lead-acid, nickel-cadmium (NiCd) and nickel-metal hydride (Ni-MH) batteries, whose cycle-life vs. DOD curve has an exponential shape. It is not, however, suitable for many lithium-based cells, whose cycle-life vs. DOD curve sometimes exhibits a more linear behavior (e.g., for $LiFePO_4$ cells).
A slightly different relationship between cycle-life and DOD was introduced in [10]:

$$N = N_{0.8} \cdot DOD' \cdot e^{\alpha \cdot (1 - DOD')} \tag{3}$$

where $N_{0.8}$ is the cycle life at $DOD = 80\%$, while α is a constant whose value is, respectively, 3 and 2.25 for lead-acid and Ni-MH tested battery packs.
Thaller [11] has defined another relationship for battery cycle life after considering excess capacity F, with respect to the rated capacity, and a penalty factor due to the DOD, by including the P parameter, as reported in (4), which gives this mathematical prediction model for a general battery:

$$N = \frac{1 + F - DOD'}{A \cdot (1 + P \cdot DOD') \cdot DOD'} \tag{4}$$

In our work, F is always considered equal to 0, so that each analysis is performed after starting from the rated capacity of any commercial cell or cell string. The product $A \cdot DOD'$ represents the irreversible capacity loss in each cycle. Values of the parameter A were originally declared to be in the range $0.000 \div 0.002$ [11].
These previous models estimate the cycle life of a battery, always after considering a fixed irreversible capacity fading (e.g, 20%, that is, when the total maximum available capacity reaches 80% of the nominal one).
In [12] the authors introduce a complex cycle life model consisting of different equations, one for each stress factor considered, i.e., C-rate, T and DOD. Despite its high accuracy, the model derivation requires extensive empirical measurements and the model itself lacks the compactness and the generality of a Peukert-like equation.

Another analytical method for battery life prediction is based on the *ampere-hour throughput*, i.e., the total energy supplied by the battery during its life [13], also called "charge life". The charge life Γ_R in ampere-hours (Ah) is defined as:

$$\Gamma_R = L_R \cdot DOD' \cdot C_R \tag{5}$$

where C_R is the rated capacity in *Ah* at a rated discharge current I_R, and L_R is the maximum number of cycles referring to a given normalized depth of discharge DOD' and a discharge current I_R. In the model presented in [14], the authors proposed calculating an equivalent *Ah* weighted-throughput parameter.
The model proposed in [15] adopted this approach to estimate the cycling capacity fade through a modified definition of the Arrhenius equation, characterized by a square root time dependence.

2.3 Motivations for the Work

Nowadays, with the remarkable rise in the production of battery-powered electronic devices, system-level design requires an analysis of both circuit and power supply in order to optimize the entire system [1]. Furthermore, battery technology is always "work in progress", as novel battery chemistries are continuously proposed. For instance, during the last two decades Li-ion batteries have mostly replaced NiCd and Ni-MH batteries in mobile phones and portable computers, mainly due to a greater specific energy (Wh/kg) [20].
Therefore, although various models have been proposed in the literature for specific battery types, a more general and flexible model for different chemistries, but still simple enough for fast characterization and simulation, is required.
In spite of the various differences, all the aforementioned models reported in Section 2.2 are built by extracting parameter values through measurements on the batteries under test. Although the generated models are typically very accurate, this approach is quite time-consuming (especially when multiple cycles are involved) and requires expensive laboratory instrumentation.
There are other methods for analyzing cycle life through computer simulation [21], but they consider the complex governing equations of the chemical reactions. For this reason, methods that only rely on available manufacturer data (e.g., datasheets) to derive the capacity fade in batteries using analytical models (e.g., [22]) or equivalent electrical circuits (e.g., [23]) have been reported in the literature in recent years. Clearly, the accuracy of these models depends on the amount of available information reported in battery datasheets.
The main result of this work is to provide a compact model [24], which expresses *the number of usable cycles as a function of the DOD*, extended for including the other factors affecting capacity fade, namely temperature and charge/discharge current.
The basic outcome of the characterization is a N vs. DOD curve, such as the one shown in Fig. 1. This information is seldom available in typical datasheets and has to be extracted by building an analytical model according to the methodology described in the next section. Needless to say, for the rare cases in which this information is available in the datasheet, the plot can be used directly without resorting to our method. However,

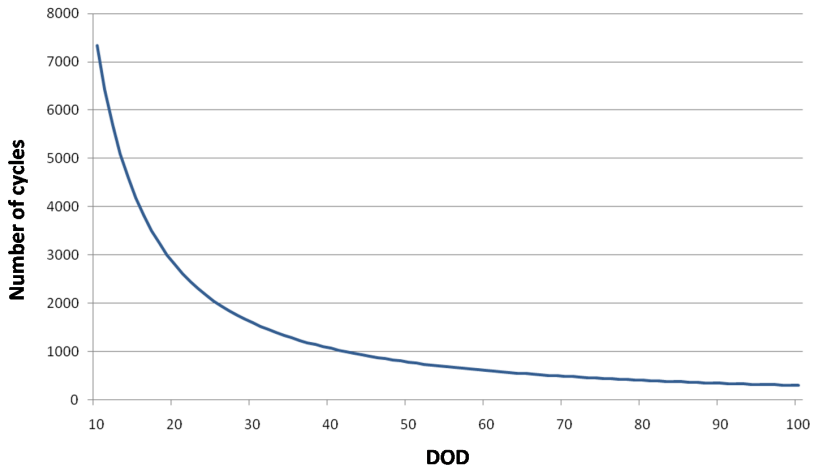

Fig. 1. A typical plot of *Number of cycles vs. DOD*.

in this work we will also consider batteries whose datasheets provide this information, in order to validate our proposed model.

3 Modeling Methodology

3.1 Model Definition

The model proposed in this work somehow mimicks the shape of Peukert's law, as expressed by (6), which models the *intra-cycle* non-linear dependency between capacity and the discharge current:

$$t = \frac{C}{I^k} \tag{6}$$

where C is the capacity of the battery, I is the discharge current, and t is the time for totally discharging the battery; k is the Peukert coefficient; typical values of k depend on the battery chemistry and the manufacturing process and they typically range from 1.1 to 1.3. As a matter of fact, the curves describing the *Capacity vs. Number of cycles* exhibit a similar non-linear relationship.

Our objective is therefore to derive a model expressing battery cycle life in a compact mathematical form similar to Peukert's law, and describing the general non-linear relationship between the capacity fade and the DOD.

In the case of capacity fade, the non-linearity concerns both the number of cycles N as well as the DOD, and the actual relationship among these quantities depends also on the value of the target capacity degradation (i.e., the behavior for a 20% capacity fade will be different from that for a 30% capacity fade). In order to model this non-linearity we need to define a new parameter that characterizes the battery performance during the cycling.

The proposed mathematical model is shown in (7); it allows to estimate the number of charging-discharging cycles N for a given battery based on four main parameters.

$$N = L \cdot \frac{C_{fade}}{DOD^h} \tag{7}$$

- L (called the *empirical factor*) is the parameter that is used to calibrate the second term of the model with respect to the number of cycles.
- C_{fade} is the percentage of irreversible capacity loss for which battery life: usually it is considered as 20%, but some manufacturers considers a different value (e.g., 30 %).
- DOD is the depth of discharge expressed as a percentage (eg. 50%); to avoid division by 0, it must be > 0, so its range is 1–100%.
- h is the coefficient that models the nonlinear relationship between N and DOD for a certain C_{fade}.

The similarity with Peukert's law is evident. N, considered as an *inter-cycle* "lifetime" parameter, is obtained as the ratio of capacity fade and a weighted metric of the rated capacity discharged on average per cycle (DOD^h). There are however two relevant differences: (i) factor L is used to scale the "lifetime" across multiple cycles, and (ii) h is not constant, but depends on C_{fade}. This makes our approach more general with respect to previous models and allows one to adapt it to the available manufacturer's data. In fact, the proposed model have two degree of freedom, i.e., L and h, while in the aforementioned models in equations (2), (3), and (4) reported in Section 2, one of the two parameters is always fixed because it is strictly related to a physical characteristic, while only the other might be set in order to fit the cycle life function.
Concerning the typical range of DOD, most manufacturers avoid using very low values of DOD (which will results in very large values of N, besides being unrealistic) and usually provide data for DOD in the range from 10–30% to 80–100% [25]. Moreover, in case of only a few cycles in a long period of time, aging is usually more influenced by calendar life than cycle life.
The model of Equation (7), by defining a generic model template, is adaptable also to some batteries like some $LiFePO_4$ batteries, which report a strictly linear *Capacity vs. Number of cycles* characteristic; for this battery, a value of h closer to 1 will easily fit easily the linear dependency.

3.2 Analysis of the Mathematical Model

In Equation (7), C_{fade} is constant, and fixed to a standard value, i.e., 20% as in typical datasheets. Besides the "physical" quantities (C_{fade} and DOD), the model includes two other scale parameters, i.e., the empirical factor L and the binding coefficient h, which have to be determined by fitting empirical data derived from available information (e.g., datasheet). These two parameters reflect a specific characteristic of the battery behavior during its cycle life.
The empirical factor L usually has a value with an order of magnitude comparable to the value of N at low (e.g., 10 or 20%) DODs. In other words, we can see L as a factor that calibrates the value of the second term of the model (the fraction). Since C_{fade} is

constant for a given battery, the fraction actually reduces to $1/DOD^{h}$. By plotting this expression as a function of the DOD (Figure 2) for different values of h, we can clearly see how the non-linearity of $1/DOD^{h}$ is modulated quite markedly by h. For large (≥ 1) values of h, the curve tends to flatten out, implying that the fraction $1/DOD^{h}$ tends to become independent of DOD, and relatively low (< 0.1). Smaller values of h, conversely, emphasize the dependency on DOD, resulting in significant differences (in order of 0.15–0.2) between low and high DOD values.
The analysis also implies that it is not possible to extract this factor only by analyzing the battery *inter-cycle* behavior, so an algorithm should be run in order to find the two parameters L and h generating the model that best fits the battery cycle life characteristic.

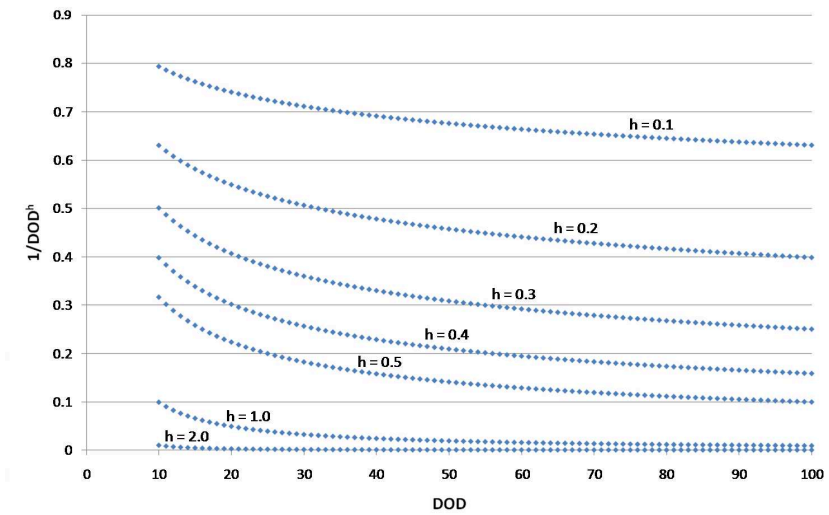

Fig. 2. $1/DOD^{h}$ *vs. DOD* for different h values.

In the next section we present such an algorithm, which searches for the values of both L and h that populate the model having the minimum error in the cycle life estimation with respect to the actual data.

3.3 Extraction of Model Parameters

The actual parameter identification depends on the amount of available data. Many manufacturers provide information about capacity fade in the form of a *Capacity vs. Number of cycles* curve as also depicted in Fig. 3. From these plots, it is no simple matter to perform the battery cycle life evaluation, since the data about the number of cycles are available for a given number of DODs only (e.g., [16]) and, furthermore, sometimes they might even show an uncertainty that may range from 8 to 10%, or even higher.

As discussed in Section 2, our model is meaningful if the battery under analysis only provides information in the form of two or more curves in the (capacity, number of cycles) plane, each corresponding to a different DOD.
Let us assume that there are M such curves available in a datasheet or in a measured set of data. Obviously the larger M, the more accurate the fitting process will be. Fig. 3 exemplifies this scenario.

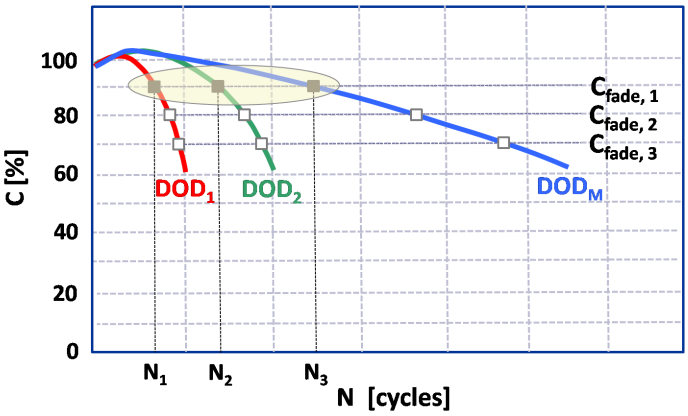

Fig. 3. Model Extraction Scenario.

Since we need to determine two parameters from the curve(s) (h and L), and given the limited number of samples points to be considered, it is feasible to derive them from an exhaustive exploration for all C_{fade} and DOD points, as the values of h and L that minimize the maximum error with respect to the curves. However, an exploration requires a feasible range for these two parameters, which is not easy to determine because they are only weakly linked to "physical" quantities. Of the two, L is the one with some physical interpretation since it can be regarded as a correction factor of the number of cycles N. Therefore, we can assume that L ranges between 1 and a value L_{max}, determined by inspection of the datasheet. As a rule of thumb, it is usually near to the largest value of N reported in the datasheet curves. Conversely, we have no insight of possible values of h. For this reason, we implement the search as a two-phase process, as described by Algorithm 1.
The search is organized into of two main iterations over L. In the first one (Lines 1–7), for all values of C_{fade} (assumed to be discretized into P values) and of the M DOD values it computes the resulting value of h using (8), which is simply a re-arrangement of (7) expressing h instead of N, and determines thus a feasible range $\mathscr{H} = [h_{min}, h_{max}]$ for h.

$$h = \frac{log(L \cdot \frac{C_{fade}}{N})}{log(DOD)} \tag{8}$$

Now that we have a feasible range for h, in the second iteration (Lines 10–26), we determine the optimal values of h and L, as follows. In the outer loop over L (Line 10),

Algorithm 1 Search for the best value of L

```
for all L ∈ [1, L_max] do
    for all C_fade = 1...P do
        for all DOD = 1...M do
            Compute h by (8)
        end for
    end for
end for
𝒽 ← [h_min, h_max]
MinMaxErr ← ∞.
for all L = 1...L_max do
    MaxErr ← 0.
    for all h ∈ 𝒽 do
        TotErr ← 0, MinAvgErr ← ∞.
        for all C_fade = 1...P do
            for all DOD = 1...M do
                Calculate N using (7) and compute the
                absolute error E
                TotErr ← TotErr + E
            end for
        end for
        AvgErr ← TotErr/(P * M)
        if AvgErr < MinAvgErr then
            H[L] ← h
            Err[L] ← AvgErr
        end if
    end for
end for
L_opt ← argmin(Err)
h_opt ← H[L_opt]
```

the optimal value of h is calculated first; for each value of h (using some discretization step), C_{fade} and DOD, N is computed using the model equation (7) (Line 16), and the error between this value and the one extracted from the datasheet is evaluated. The value of h that yields the least average error is stored as the best for a given value of L into an array **h**, together with the relative errors (array **Err**, Lines 22-23).
At the end of the iteration over L, the value of L corresponding to the smallest error is selected as single L_{opt} for the model (Lines 27-28), which is used as an index in **h** to determine h_{opt} for each C_{fade}.

4 Model Validation

The validation of the proposed model is performed after considering batteries of various chemistries produced by different manufacturers. Although the type of aging data may differ from one datasheet to another, we have collected the available information and translated it into the tabular format described in Section 3; using these data, we ran the search algorithm to populate the model for each battery under analysis.

4.1 VRLA Batteries

We start our evaluation from Valve Regulated Lead Acid (VRLA) batteries, which have a more evident nonlinear aging behavior with respect to many other chemistries. Moreover, datasheets for most VRLA batteries include more detailed information on aging, typically in the form of the plot of $Capacity\ vs.\ Number\ of\ cycles$ (e.g., Fig. 3).
Table 1 reports the extracted manufacturer data and the resulting model parameters for two different Absorbed Glass Mat (AGM) VRLA batteries: the XTV1272 by CSB Battery and the EV12A-B by DISCOVER®. The first three columns represent the data given from the related datasheets, in both cases for three different C_{fade} points, namely 10, 20, and 40%. The last four columns report the parameters obtained by the search algorithm, the resulting number of cycles N_m from the model, and the estimation maximum absolute error. After comparing N_m against the cycle life extracted from the datasheets (i.e., N_d), the greatest errors are given for a low (i.e., 10%) C_{fade}, while they are fairly small for typical lifespan (i.e., C_{fade} = 20% or greater).
Although the error is not negligible, it is worth emphasizing that very often datasheets report a possible range of the number of cycles rather than a single curve, to indicate the intrinsic uncertainty of the estimation. The spread of the values actually increases for increasing DODs. For instance, from the datasheet for the XTV1272 [16], we found that the possible variation of the cycle life (measured as the difference between the minimum or maximum value with respect to the average) might even be up to 10, 11, and 16% for $C_{fade} = 10, 20,$ and 40%, respectively. Hence, the absolute **maximum** estimation error obtained by the proposed model (i.e., around 12, 11, and 12%, respectively) is comparable with the maximum tolerance given by the manufacturer.

4.2 Other Battery Chemistries

Evaluation of other battery chemistries is complicated by the fact that in general only the manufacturers of VRLA batteries provide plots of $Capacity\ vs.\ Number\ of\ cycles$,

Table 1. Extracted parameters and number of cycles estimation for the CSB XTV1272 and DISCOVER EV12A-B AGM-VRLA batteries.

Battery	*Datasheet*			*Model*			
	N_d	*DOD*	C_{fade}	*L*	*h*	N_m	*Max. error* (%)
CSB XTV1272	681	30	10	2464	1.093621	597	-12.33
	305	50				342	12.13
	151	100				160	5.96
	861	30	20		1.222672	770	-10.57
	374	50				412	10.16
	186	100				177	-4.84
	1130	30	40		1.343506	1021	-9.65
	459	50				514	11.98
	231	100				203	-12.12
DISCOVER EV12A-B	1321	20	10	2691	0.961111	1512	14.46
	734	50				627	-14.58
	348	80				399	14.66
	953	20	20		1.075976	2143	9.73
	885	50				800	-9.60
	455	80				482	5.93
	2949	20	40		1.193213	3017	2.31
	1071	50				1011	-5.60
	545	80				577	5.87

for different DODs. In particular, datasheets usually report only a single curve referring to a single DOD value for lithium-based batteries. The availability of just one DOD reference, however, would yield a model with little practical use in this case, since the calibration for discharge patterns would be different from that used for characterization.

Therefore, in order to have a more meaningful assessment of the accuracy of the proposed model, we only selected those batteries whose datasheets report the *Number of cycles vs. DOD* characteristic, even just for a single C_{fade} value. In any case, values of *DOD* below 10% are not used for the derivation of the model because (i) they are not representative of typical battery usage and (ii) they are not statistically representative. It is worth noticing that the number of cycles should approach infinity as $DOD \rightarrow 0\%$; therefore, as *DOD* gets smaller it would be correct to consider a range of values rather than a precise value. Of course, all the characteristics given by the manufacturers always refer to certain operating and working conditions (e.g., charge/discharge current and temperature), which are usually different from one brand to another. In order to validate the basic proposed model, at the beginning we do not consider the differences among these conditions. However, both temperature and current rate, as stress factors in battery aging, are included in the extended model as reported in Section 5.

The parameters and estimation errors for the benchmark batteries are reported in Tables 2 and 3, which also report, for a more comprehensive validation, the results of the application of the existing and most meaningful analytical models [9, 11]. As (2) requires the number of cycles at DOD=100% as input parameter, the evaluation of that previous model was not possible for two batteries because this value is not available in their

datasheets, as reported in Table 2. On the other hand, as the model proposed by [11] is useless for $DOD' = 1$ (in this case, N in (4) would be equal to zero), the analysis was re-performed by considering the maximum DOD=80% as reported in Table 3.

In Table 2, the largest absolute estimation error of the model occurs for a $LiFeMgPO_4$ battery, almost 20%, while the maximum mean value is 11.35% for the Alpha® one. However, the total average error of the maximum errors for the 10 batteries in the table is 10.66%. The mean errors are obviously smaller, in general less than 10%, and in one case 11.35%.

In general, the proposed model shows robustness and accuracy for different types of electric storage devices. For the Li-ion battery by Saft Evolion the linear factor L is very high with respect to any other battery. In fact, the linear factor usually depends on the battery properties of cycling, while the range of the h parameter strictly depends on the linearity of the cycle life with respect to the DOD. The lowest h coefficient found in the model validation is 0.225627 for the Discover 22-24-700 battery, whereas the highest h is 2.000414 for the Saft Evolion.

In order to give a more comprehensive example about accuracy, Fig. 4 shows the plots obtained from all the information in the datasheet for the Lithium Manganese Dioxide Maxell ML2016 battery, and the estimation data produced by the proposed model.

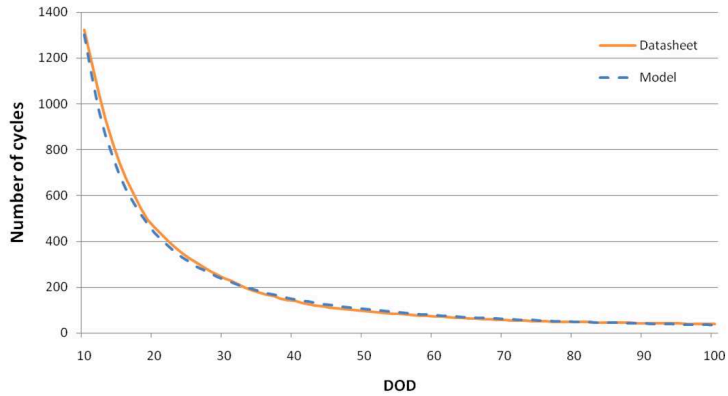

Fig. 4. Extracted N *vs*. DOD plots for the Lithium Manganese Dioxide Maxell ML2016 battery.

Fig. 5 reports the plots, normalized to the C_{fade} and parameter L, of the models for the selected batteries. The plot for the DISCOVER 22-24-6700, whose model has h = 0.225627, is reported separately in the upper right pane for the sake of clarity. The others are represented in a descending order of the h parameters reported in the fifth column of Table 2, i.e., the curve for the lowest value (0.995693) is at the top while the one for the highest value (2.000414) is at the bottom.

At the end, the chart in Fig. 6 reports a comparison of the estimation models after applying each of them to the benchmarks. For a comprehensive report, it also includes the main results obtained for the analysis of the model by [10], whose estimation errors are

Table 2. Battery data, prediction model parameters, and estimation error of the cycle life for various batteries whose manufacturers provide the Number of cycles vs. DOD characteristic.

Producer	*Code*	*Type*	*Model*							
			Proposed				[9]			
			L	h	*Abs. error [%]*		N_1	α	*Abs. error [%]*	
					max	*mean*			*max*	*mean*
EnerSys	65-PC1750	AGM-VRLA	9083	1.393212	12.34	8.05	330	2.488793	63.03	34.49
Concorde	Sun Xtender	AGM-VRLA	4629	1.176563	15.20	8.79	354	2.644044	28.56	15.73
Sonnenschein	A600	Gel-VRLA	3874	1.020317	2.03	0.92	718	1.747624	21.12	12.84
Alpha Tech.	KL, KM, KH types	*NiCd*	31107	1.587189	18.10	11.35	463	2.412794	54.04	28.38
C&D Tech.	LI TEL 48-170 C	Li-ion	109882	1.420135	6.27	3.60	2987	2.022832	2.53	1.22
Saft	Evolion	Li-ion	1157452	2.000414	13.84	8.15	n.a.	-	-	-
Seiko (SII)	MS621	$Mn\ Si\ Li-ion$	986	0.995693	0.90	0.38	202	1.712398	20.29	12.07
Maxell	ML2016	Li/MnO_2	2393	1.566125	11.28	6.49	39	2.743101	65.11	36.81
Discover	22-24-6700	$LiFePO_4$	671	0.225627	6.99	4.36	n.a.	-	-	-
Valence	U-CHARGE	$LiFeMgPO_4$	153425	1.491094	19.66	9.21	2679	2.764444	19.10	12.31

Note. n.a.: not available

Table 3. Battery data, prediction model parameters, and estimation error of the cycle life for various batteries whose manufacturers provide the Number of cycles vs. DOD characteristic. The maximum DOD is 80% for all the analyses.

Producer	*Code*	*Type*	*Model*							
			Proposed				[11]			
			L	*h*	*Abs. error [%]*		*A*	*P*	*Abs. error [%]*	
					max	*mean*			*max*	*mean*
EnerSys	65-PC1750	AGM-VRLA	9083	1.393212	12.34	7.49	0.00140	-0.436228	36.57	22.68
Concorde	Sun Xtender	AGM-VRLA	4629	1.176563	15.19	8.81	0.00180	-0.953029	8.37	5.44
Sonnenschein	A600	Gel-VRLA	3874	1.020317	2.03	0.82	0.00140	-1.010028	3.64	0.99
Alpha Tech.	KL, KM, KH types	*NiCd*	31107	1.587189	18.10	10.70	0.00110	-0.674032	13.67	7.29
C&D Tech.	LI TEL 48-170 C	Li-ion	109882	1.420135	6.26	4.21	0.00020	-0.864030	9.94	4.43
Saft	Evolion	Li-ion	1157452	2.000414	13.84	8.15	0.00010	-0.452045	59.81	34.84
Seiko (SII)	MS621	$Mn\ Si\ Li-ion$	986	0.995693	0.90	0.40	0.00500	-0.999028	0.99	0.42
Maxell	ML2016	Li/MnO_2	2393	1.566125	11.28	6.53	0.00500	1.228006	48.20	32.71
Discover	22-24-6700	$LiFePO_4$	671	0.225627	6.99	4.36	0.00060	-1.200934	52.83	38.52
Valence	U-CHARGE	$LiFeMgPO_4$	153425	1.491094	19.66	8.80	0.00020	-0.967028	27.47	15.69

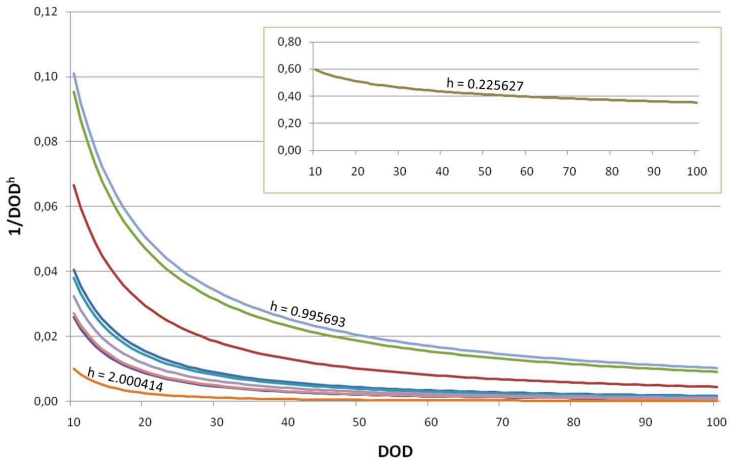

Fig. 5. $1/DOD^h$ *vs*. *DOD* of the generated models for the selected batteries.

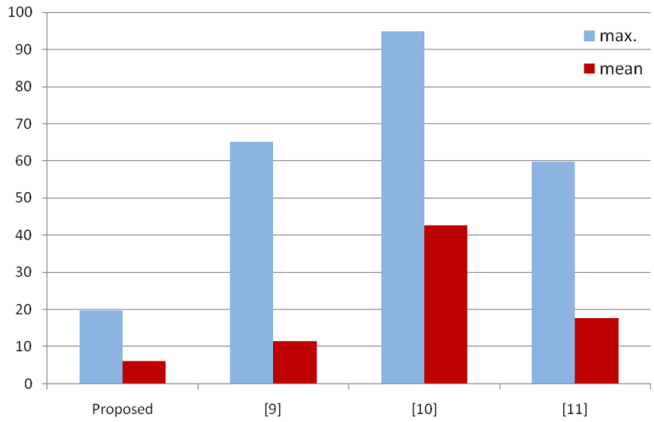

Fig. 6. Maximum and mean estimation errors given by the models for all the selected benchmarks.

too great to be reported. Furthermore, for the here proposed model, this chart considers the worst case (i.e., data reported in Table 2).

Although the previous models have two parameters (i.e., coefficients) in their expressions, one of them always strictly depends on the battery properties. In the here proposed model, both parameters L and h can be characterized, resulting in higher accuracy thanks to an additional degree of freedom in the modeling process.

5 Extension of the basic model

This Section provides an overview of temperature and current as stress factors that may accelerate the aging of batteries, and presents an extended version of the model reported in Section 3.1, in order to also include the dependency of the cycle life on these stress factors.

In this context, the total battery cycle life is the number of cycles that a battery may guarantee at different temperatures and current rates.

5.1 Impact of the Temperature on Cycle Life

The battery capacity is strongly dependent on temperature and it is not always a monotonic function. Furthermore, such a dependency changes for different battery chemistries [20].

Temperature effects on battery performance may manifest themselves in a reversible change of the total battery capacity in a single cycle, and in an irreversible capacity fading during the battery cycle life.

In the literature, an Arrhenius-type equation typically describes the relationship between battery aging due to cycle life and temperature (T) [15, 22]. For fixed values of charge and discharge C-rates, this analyitical model can be written as follows [23]:

$$C_{fade} = B \cdot e^{-E_a/(R_g \cdot T_b)} \cdot A_h^z \quad (\%) \tag{9}$$

In (9), B is a constant, T_b is the battery temperature (K), while E_a and R_g are, respectively, the activation energy (J·mol^{-1}) and the universal gas constant (i.e., 8.3143 J·mol^{-1}·K^{-1}); A_h is the total ampere-hour throughput processed after a certain number of cycles (i.e., given by $N \cdot DOD' \cdot C_R$), while z is the power law factor. Regarding the latter, [15] reports that z is always near 0.5 for a graphite-$LiFePO_4$ cell, being "fairly constant at all C-rates". In addition, this work provides all the exact values of the coefficients in (9) for a certain battery cell under test. Furthermore, it should be pointed out that both input and output ampere-hour throughputs due to charge and discharge currents, respectively, contribute to capacity fading [14].

Although equations based on Arrhenius' law provide reference analytical models, nowadays batteries may have different characteristics. In fact, there are batteries for which temperature effects, in service and cycle life, do not exactly follow Arrhenius' law. For instance, the handbook for the Sonnenschein® A600 Gelled Electrolyte (GEL) VRLA battery [26] reports a better performance with respect to Arrhenius' law, from the test results, after comparing the temperature effects on both service and cycle life. Therefore, a more adaptive model that fits any characteristics concerning capacity fading should be considered when analyzing the effect of the temperature in different battery chemistries and products.

Since (9) refers to the capacity loss due to the effect of temperature in cycle life, in order to obtain a similar equation for the calendar (service) life, the term A_h in (9) must be replaced with the battery lifetime t (months) [15, 22].

The Proposed Model for Temperature Effect on Aging

In order to include the temperature effect in the model, we consider a slightly different mathematical expression with respect to the model given in (7), but still with only two parameters, for extracting the temperature derating factor (TDF), as given by the following equation:

$$TDF = L_T \cdot \left(\frac{T_b}{T_{ref}}\right)^{h_T} + (1 - L_T) \tag{10}$$

In (10), T_{ref} is the temperature at which the model in (7) refers to (e.g., 25°C), while T_b is the battery temperature; L_T is an empirical constant, which appears two times in the formula, while h_t is the power factor that reflects the characteristic of the battery cycle life for different temperatures. Notice that the TDF is a non-negative value; it is in fact determined by the values of h_t and L_T using the algorithm of Section 3 to empirically fit the curve of N vs. T, which obviously represents a non-negative value.

5.2 Impact of the Current on Cycle Life

In various battery aging models, current is not usually considered as one of the main stress factors in cycle life (e.g., [5]). For instance, in [14] the authors claimed that the C-rate effect on aging is negligible in Li-ion cells for relatively large C-rates (in a range ±4C). This assumption cannot however be generalized for all applications and batteries. In fact, various datasheets report a different cycle life for different charge/discharge currents. For this reason, the authors in [27] proposed an extended version of Millner's aging model [5] by including both charge/discharge C-rates with their related coefficients, as extracted from the manufacturer's data for a commercial $LiFePO_4$ battery.
So, with respect to the aforementioned expression reported in (9), [15] provides a similar Arrhenius-type equation that includes the current rate (for values greater than C/2), here rewritten as follows:

$$C_{fade} = B(i_{rated}) \cdot e^{(-E_a + k_1 \cdot i_{rated})/(R_g \cdot T_b)} \cdot A_h^z \quad (\%) \tag{11}$$

In (11), the value of the pre-exponent factor B is different for each current i_{rated} (i.e., expressed in C-rate), while E_a and z can be set to a fitted value [15], as well as the coefficient k_1.
Since charge and discharge currents usually have a different impact on aging, coefficients values in (11) are generally different when considering the charge and discharge phases.

The Proposed Model for Current Effect on Aging

The discharge current derating factor (DDF) is given by the following expression:

$$DDF = L_{i_d} \cdot \left(\frac{i_d}{i_{d_{ref}}}\right)^{h_d} + (1 - L_{i_d}) \tag{12}$$

where $i_{d_{ref}}$ is the current (in C-rate value) to which the model in (7) refers, and $i_{d_{rated}}$ is the discharge current rate; L_{i_d} is an empirical factor, and h_d is the power factor that reflects the characteristic of the battery cycle life for different discharge rates.

Similarly, the charge current derating factor (CDF) is given by the following equation:

$$CDF = L_{i_c} \cdot \left(\frac{i_c}{i_{c_{ref}}} \right)^{h_c} + (1 - L_{i_c}) \tag{13}$$

where $i_{c_{ref}}$ is the charge current (in C-rate value) to which the model in (7) refers to, while i_c is the discharge current; similar to the previous expression in (12), L_{i_c} and h_c are the parameters for characterizing the battery behavior for different charge rates.
Finally, the full equation for analyzing the battery cycle life as a function of DOD, T, and C-rate, is given by the following formula:

$$N(DOD, T, i) = L \cdot \frac{C_{fade}}{DOD^h} \cdot TDF \cdot DDF \cdot CDF \tag{14}$$

In (14), both the derating factors for charge and discharge currents must be included because generally they have a different impact on battery aging and, therefore, different coefficients in their formulas.

5.3 Results

Preliminary results are obtained for the Sonnenschein A600 GEL-VRLA and Discover 22-24-6700 $LiFePO_4$ batteries, as their datasheets provide enough information for modeling their cycle life considering temperature effects. For both batteries, the analysis was conducted considering a maximum T_b equal to 50°C.
Table 4 reports the extracted h_T parameter for each battery, and the estimation errors of the temperature derating factor given by the model in (10) with respect to the manufacturers' data.

Table 4. Extracted parameters of the derating factor for the model extended to the **temperature** effect in cycle life, and consequent estimation error of the model with respect to the manufacturers' data.

Producer	*Code*	*Type*	L_T	h_T	*Max. error* (%)	*Mean error* (%)
Sonnenschein	A600	Gel-VRLA	2.99	-0.391034	9.77	3.87
Discover	22-24-6700	$LiFePO_4$	2.13	-0.840028	8.44	3.23

It is worth noticing that in both cases the maximum error is less than 10%.

As far as concerns the current effect on battery aging, which is usually considered for high C-rates only, the model given in (12) was applied to the Discover 22-24-6700 $LiFePO_4$ battery, for which the extracted parameters L_{i_d} and h_d are, respectively, 0.98 and -0.851245. In this case, the maximum and mean estimation errors are, respectively, 2.36% and 0.96%. These results demonstrate the high level of accuracy that the proposed extended model may guarantee.

6 Conclusion

A compact mathematical model for estimating the number of cycles of a battery with respect to an expected capacity fade, has been proposed. The related equation describes the cycling behavior of batteries of different chemistries, and it demonstrates the possibility of obtaining a very fast and also accurate exploration of battery lifespan. The characterization of the long-term effects for a specific battery only requires two battery-specific parameters: an empirical factor L and the exponential h coefficient. Validation results show an estimation mean error generally within 10%.
Furthermore, the basic model has been extended to include temperature and current rate effects in battery cycle life. In this scenario, various derating factors have been defined using mathematical models similar to the basic one. The mean absolute estimation errors of these models related to temperature and discharge current are, respectively, less than 4% and about 1%.

References

1. Benini, L., Castelli, G., Macii, A., Macii, E., Poncino, M., Scarsi, R.: Discrete-Time Battery Models for System-Level Low-Power Design. Transactions on Very Large Scale Integration (VLSI) Systems, vol. 9, no. 5, pp. 630–640. IEEE, (2001)
2. Chen, M., Rincón-Mora, G.A.: Accurate Electrical Battery Model Capable of Predicting Runtime and I-V Performance. Transactions on Energy Conversion, vol. 21, no. 2, pp. 504–511. IEEE, (2006)
3. Petricca, M., Shin, D., Bocca, A., Macii, A., Macii, E., Poncino, M.: An Automated Framework for Generating Variable-Accuracy Battery Models from Datasheet Information. In: International Symposium on Low Power Design, pp. 365–370. IEEE/ACM, (2013)
4. Peukert, W.: Über die Abhängigkeit der Kapazität von der Entladestromstärke bei Bleiakkumulatoren. Elektrotechnische Zeitschrift, vol. 20, pp. 20–21. (1897)
5. Millner, A.: Modeling Lithium Ion battery degradation in electric vehicles. In: Conference on Innovative Technologies for an Efficient and Reliable Electricity Supply, pp. 349–356. IEEE, (2010)
6. Ramadass, P., Haran, B., White, R., Popov, B.N.: Mathematical modeling of the capacity fade of li-ion cells. Journal of Power Sources, vol. 123, no. 2, pp. 230–240. Elsevier, (2003)
7. Lam, L., Bauer, P.: Practical Capacity Fading Model for Li-Ion Battery Cells in Electric Vehicles. Transactions On Power Electronics, vol. 28, no. 12, pp. 5910–5918. IEEE, (2013)
8. Ramadesigan, V., Chen, K., Burns, N.A., Boovaragavan, V., Braatz, R.D., Subramanian, V. R.: Parameter Estimation and Capacity Fade Analysis of Lithium-Ion Batteries Using Reformulated Models. Journal of the Electrochemical Society, vol. 158, no. 9, pp. A1048–A1054. ECS, (2011)
9. Seiger, H.N.: Effect of Depth of Discharge on Cycle Life of Near-Term Batteries. In: 16th Intersociety Energy Conversion Engineering Conference, pp. 102–110. American Society of Mechanical Engineers, (1981)
10. Burke, A.F.: Cycle Life Considerations for Batteries in Electric and Hybrid Vehicles. Technical paper, No. 951951. SAE, (1995)
11. Thaller, L.H.: Expected Cycle Life vs. Depth of Discharge Relationships of Well-Behaved Single Cells and Cell Strings. Journal of Electrochemical Society, vol. 130, no. 5, pp. 986–990. ECS, (1983)

12. Omar, N., Monem, M.A., Firouz, Y., Salminen, J., Smekens, J., Hegazy, O., Gaulous, H., Mulder, G., Van den Bossche, P., Coosemans, T., Van Mierlo, J.: Lithium iron phosphate based battery – Assessment of the aging parameters and development of cycle life model. Applied Energy, vol. 113, pp. 1575–1585. Elsevier, (2014)
13. Symons, P.: Life Estimation of Lead-Acid Battery Cells for Utility Energy Storage. In: Fifth International Conference on Batteries for Utility Storage. Puerto Rico Electric Power Authority, (1995)
14. Marano, V., Onori, S., Guezennec, Y., Rizzoni, G., Madella, N.: Lithium-ion batteries life estimation for plug-in hybrid electric vehicles. In: Vehicle Power and Propulsion Conference, pp. 536–543. IEEE, (2009)
15. Wang, J., Liu, P., Hicks-Garner, J., Sherman, E., Soukiazian, S., Verbrugge, M., Tataria, H., Musser, J., Finamore, P.: Cycle-life model for graphite-LiFePO4 cells. Journal of Power Sources, vol. 196, no. 8, pp. 3942–3948. Elsevier, (2011)
16. CSB Battery Co., Ltd. `http://www.csb-battery.com/upfiles/dow01404206487.pdf` (accessed January 7, 2016).
17. Vetter, J., Novák, P., Wagner, M.R., Veit, C., Möller, K.-C., Besenhard, J.O., Winter, M., Wohlfahrt-Mehrens, M., Vogler, C., Hammouche, A.: Ageing mechanisms in lithium-ion batteries. Journal of Power Sources, vol. 147, no. 1-2, pp. 269–281. Elsevier, (2005).
18. Broussely, M., Biensan, P., Bonhomme, F., Blanchard, P., Herreyre, S., Nechev, K., Staniewicz, R.J.: Main aging mechanisms in Li ion batteries. Journal of Power Sources, vol. 146, no. 1, pp. 90–96. Elsevier, (2005)
19. Bashash, S., Moura, S.J., Fathy, H.K.: Charge Trajectory Optimization of Plug-in Hybrid Electric Vehicles for Energy Cost Reduction and Battery Health Enhancement. In: 2010 American Control Conference, pp. 5824–5831. IEEE, (2010)
20. Reddy, T.B.: An Introduction to Secondary Batteries. In: Linden, D., Reddy, T.B. (eds.) Linden's Handbook of Batteries, Fourth Edition. McGraw-Hill Co., (2011)
21. Ning, G., White, R.E., Popov, B.N.: A generalized cycle life model of rechargeable Li-ion batteries. Electrochimica Acta, vol. 51, no. 10, pp. 2012–2022. Elsevier, (2006)
22. Spotnitz, R.: Simulation of capacity fade in lithium-ion batteries. Journal of Power Sources, vol. 113, no. 1, pp. 72–80. Elsevier, (2003)
23. Petricca, M., Shin, D., Bocca, A., Macii, A., Macii, E., Poncino, M.: Automated generation of battery aging models from datasheets. In: 32nd IEEE International Conference on Computer Design, pp. 483–488. IEEE, (2014).
24. Bocca, A., Sassone, A., Shin, D., Macii, A., Macii, E., Poncino, M.: An equation-based battery cycle life model for various battery chemistries. In: 2015 IFIP/IEEE International Conference on Very Large Scale Integration, pp. 57–62. IEEE, (2015)
25. Broussely, M., Herreyre, S., Biensan, P., Kasztejna, P., Nechev, K., Staniewicz, R.J.: Aging mechanism in Li ion cells and calendar life predictions. Journal of Power Sources, vol. 97, pp. 13–21. Elsevier, (2001)
26. GNB Industrial Power: Sonnenschein®: Handbook for Stationary Gel-VRLA Batteries Part 2: Installation, Commissioning and Operation. Edition 17. Exide Technologies, (2012)
27. Bocca, A., Sassone, A., Macii, A., Macii, E., Poncino, M.: An aging-aware battery charge scheme for mobile devices exploiting plug-in time patterns. In: 33rd IEEE International Conference on Computer Design, pp. 407–410. IEEE, (2015).